ARCHIVES OF MECHANICS
Arch. Mech. **75** (1-2), 151–168, 2023, DOI: 10.24423/aom.4064

A numerical approach in applying panel method for the added mass of a group of sections in fluids

D. ZHANG, P. LI*), Q. WANG, Y. YANG

*School of Mechanics and Engineering, Applied Mechanics and Structure Safety Key Laboratory of Sichuan Province, Southwest Jiaotong University, Chengdu, 610031, P.R. China, *) e-mails: meiyongyuandeze@163.com, lp_vib@126.com*

This paper firstly expands an efficient numerical methodology developed from the source panel method to the added mass calculation of long column systems in fluid. Structures submerged in fluid are considered as two-dimensional and are discretized into a number of source panels. The influence coefficient matrices and the potential function are then calculated and the fluid forces are calculated by the unsteady Bernoulli equation. Finally, we utilize this present method to calculate the mass coefficients of some typical problems, which effectively verifies its feasibility and accuracy. This method takes into account both applicability and computational efficiency. On the one hand, in contrast to the analytical method which is only applicable to specific cross-sections, this method is applicable to arbitrary boundaries with $\mathcal{C}^0$ continuity in mathematics. On the other hand, this method requires less mesh and computation than commercial software. This paper extends the application of the source panel method which is widely used in aerodynamics to provide a reference for added mass calculation problems in engineering.

Key words: numerical method, panel method, fluid-structure interaction, confined fluid, fluid mass coefficients.

1. Introduction

The movements of structures in fluid may cause the surrounding fluid to move, and the accelerated fluid thereby creates a non-uniform pressure field on structures. Thus structures are subjected to added fluid forces of the surrounding fluid. This problem can be found in many applications, especially in nuclear engineering, and has been regarded as a typical problem in Applied Mechanics. The fluid effect should be carefully evaluated because it can enormously change the structures of dynamic behaviors. People mainly focus on the inertia effect of the fluid, particularly in free vibration, because it is the main factor that affects the natural characteristics [1] and vibration characteristics in dynamic analysis [2] of the system. The fluid inertia effect due to the motion of a structure

can be generally quantified in terms of the mass coefficients and its moving acceleration [1, 3], the calculation of mass coefficients is of great importance in engineering.

It is usually difficult to solve the added masses of structures directly. In engineering such as heat exchanger tubes in nuclear reactors, many structures are usually long columns and the hydrodynamic problem can be considered as two-dimensional [1, 3]. This allows the solution of the added mass to be very simplified. Experiments have also verified the accuracy of two-dimensional models [4]. In a more general sense, the fluid in which these structures are immersed is restricted by other boundaries, which refers to a bounded fluid. FRITZ [4] may have been the first to propose a method for evaluating the fluid forces of two moving coaxial circles in incompressible, frictionless fluids by Lagrange's equations. The author pointed out that the method suggested for the two-sections problem can apply to multiple-body problems; however, this problem is so complex that the fluid specialist must work with the dynamics specialist to develop the solutions. CHUNG and CHEN [5] presented an analytical method for the mass coefficients of a group of circular cylinders immersed in a fluid contained in a cylinder by the series method. However, this method can only apply to the cylindrical structures submerged in a container and is unavailable for other complex sections. DONG [6] gave the mass coefficients of single elliptical, rhombic, rectangular, and H-shaped sections, but the mass coefficients of more complex cross-sections were not discussed.

For more complex structures, PAIDOUSSI [1] firstly used the self-programmed finite elements method (differentiate with the commercial finite element software like ANSYS) for the mass coefficients calculation of cylinders in a liquid-filled channels. It is shown that the finite element method is more general but is less efficient for the problem presented in [5]. In recent years, with increasing popularity of commercial software, it has also been used for the mass coefficients calculation. JEONG [7] studied the added mass effect on translational and rotation motions of a square section in the ANSYS square wall and obtained the rule of natural frequencies and the gap. This method is easy to operate, but it is difficult to calculate the coupling mass coefficients between sections themselves. LI [8] studied the added mass of spent fuel storage racks by the CFD method, and the numerical results are in good agreement with the experiment. This method can also be used to calculate the coupling added coefficient. However, it is worth noting that this method will cost lots of computing time, and updating the moving fluid grid is still a big challenge.

By summarizing the relevant literature above, we found that for the calculation of mass coefficients of two-dimensional sections, analytical and numerical methods have the advantages of efficiency and applicability, respectively. However, analytical solutions are not easily applied to more general cases due to

their limitations. The analytical methods are not suitable for complex cross-sections [4, 5], and even are inapplicable if the boundaries are not with $\mathcal{C}^1$ continuity in mathematics. The fluid finite element methods generally require complex meshing and programming work [1]. Furthermore, the CFD methods need to do enough transient analysis to finally obtain the required steady fluid force, which needs much time, and updating the fluid grids which is also a big challenge [8]. In respect of engineering practice, some new methods are still needed that can give accurate solutions at a low cost of computing and programming.

We notice that in aerodynamics, the source panel method is an efficient technique for the numerical solution of non-lifting flows over arbitrary sections and bodies in aviation [9]. It has the advantages of high efficiency and easy programming and has become a standard aerodynamic tool. This method has been widely used in the calculations of fluid forces of aircraft [10], ships and marine propellers [11, 12], racing cars [13], and plate structures [14]. It is based on replacing the section's geometry with singularity panels so it can therefore be applied to calculations with arbitrary cross-sections. These advantages of the panel method mean that it may provide an efficient method, for calculating added mass coefficients for complex sections immersed in the fluid. Based on the three-dimensional panel method, ASHBY [15] developed a low-order potential-flow panel code. This code was originally developed for the calculation of internal flow model, jet wake model, and the time-stepping wake model. SAHIN [16] had successfully extended this code to added mass calculations for two and three dimensional structures and it is found that this code can be successfully used for calculating the added masses. It is worth noting that, in [16], the authors have defined the length of the column to be very long in order to simulate the two-dimensional situation, but the calculation is actually built according to the three-dimensional model. As a result there are many elements in the length direction, which increase the number of required elements and reduce the efficiency of the calculation. In fact, for two-dimensional models, it is possible to calculate their added masses from the two-dimensional panel method. While to the best of our knowledge, there is no research literature on using it for the mass coefficients of structures in engineering, and this is the intended role of the present study.

In this technical paper, the panel method is expanded and developed to the added mass coefficient calculations of complex sections in fluids for the first time. We begin Section 2 with a general model of a group of sections with arbitrary boundaries in a confined fluid and give the fundamental equations for calculating the added mass coefficients. Moreover, this section presents a detailed numerical modeling approach to applying the panel method for the added mass coefficients. Section 3 comprehensively examines its effectiveness and accuracy by comparing the results calculated by this new numerical method and other theories and software. These validation examples are carefully selected that can cover some

typical section boundary features ($\mathcal{C}^0$ or $\mathcal{C}^1$ continuity, a single boundary, or a group of boundaries) and the fluid domain feature (open or bounded flow). Finally, some general conclusions of this study are summarized in Section 4.

2. Modeling and methodology

2.1. Model and basic equations

A generic diagram of the current system is shown in Fig. 1(a). There is a group of sufficiently long columns which can be considered as two-dimensional sections $\mathcal{A}_i$ $(i = 1, \ldots, N)$ in a sufficiently long container. The container, with an arbitrarily closed boundary $\mathcal{B}_0$, is filled with fluid. The fluid is assumed to be inviscid, irrotational and incompressible fluid, i.e. ideal fluid. It is worth noting that the fluid is assumed to be inviscid and therefore fluid added damping cannot be calculated in this method. As with much of the literature, only the added mass calculations, most relevant to the kinetic properties are considered in this paper. Each of the inner section in the container is enclosed by an arbitrarily closed boundary $\mathcal{B}_i$ $(i = 1, \ldots, N)$, and there is no fluid inside them. It is assumed that all sections are undeformed but can undergo the plane translational motions. If the container is absent, it corresponds to the case of an open fluid (infinite fluid).

As pointed out by [5], the effect on the i-th section caused by sections' motion can be calculated by the superposition principle. Assume that the j-th section is moving with the velocity $\mathbf{v}_j = (v_j^x, v_j^y)$, and all of the other boundaries are stationary. Such motion can result in a disturbance of the fluid velocity perturbation potential φ, and its control equation is written as

$$\nabla^2 \varphi = 0. \tag{2.1}$$

The above equation is the well-known Laplace equation and should be solved by the following boundary conditions:

$$\frac{\partial \varphi}{\partial \mathbf{n}_k} = \begin{cases} \mathbf{v}_j \cdot \mathbf{n}_j, & k = j, \\ 0, & k \neq j, \end{cases} \tag{2.2}$$

where $\mathbf{n}_k = (n_k^x, n_k^y)$ is the normal vector of the boundary $\mathcal{B}_k$, and v_j^x and v_j^y are the components of the velocity $\mathbf{v}_j$ in the x and y directions, respectively.

The fluid pressure p_i due to the fluid disturbance potential φ on the boundary $\mathcal{B}_i$ can be calculated by the unsteady Bernoulli equation as [5]

$$p_i = -\rho_f \frac{\partial \varphi}{\partial t}\bigg|_{\text{on } \mathcal{B}_i}, \tag{2.3}$$

where ρ_f is the fluid density. From Eqs. (2.1)–(2.3), it is known that the fluid pressure is a function of j-th section acceleration, and the fluid force on the i-th section can be calculated as:

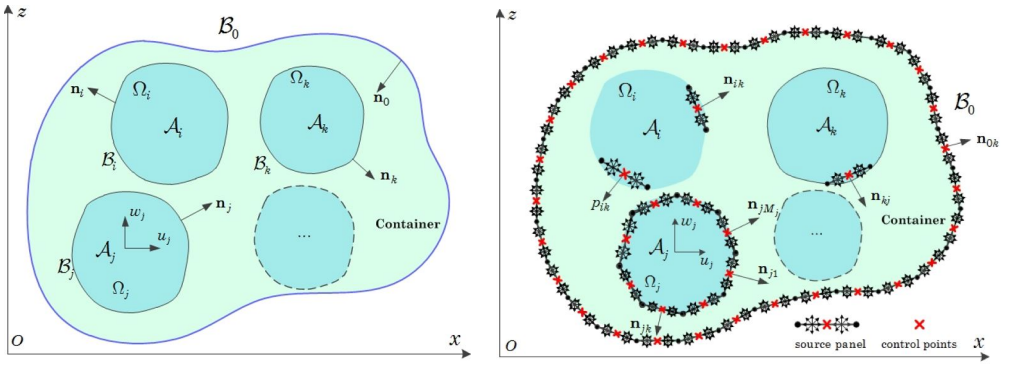

(a) (b)

FIG. 1. Sketch of (a) the model of a group of sections in a container and (b) the system discretization.

$$\begin{cases} F_{i-x} = -\oint\limits_{\mathcal{B}_i} p \cdot n_i^x \, ds = -\rho_f(\alpha_{ij} a_j^x + \sigma_{ij} a_j^y), \\ F_{i-y} = -\oint\limits_{\mathcal{B}_i} p \cdot n_i^y \, ds = -\rho_f(\tau_{ij} a_j^x + \beta_{ij} a_j^y), \end{cases} \tag{2.4}$$

where a_j^x and a_j^y are respectively the components of the acceleration of the j-th section in the x and y directions; and they are defined as

$$\mathbf{a}_j = \frac{d\mathbf{v}_j}{dt} \triangleq (a_j^x, a_j^y),$$

and $\alpha_{ij}, \sigma_{ij}, \tau_{ij}, \beta_{ij}$ are the coefficients standing for the coupling fluid inertia force between different sections. For a further evaluation, we consider that the boundary $\mathcal{B}_j$ is moving with a unit acceleration, then we can obtain the following four non-dimensional coefficients:

$$\begin{cases} m_{ij-xx} = -\dfrac{F_{i-x}(a_j^x \equiv 1, a_j^y \equiv 0)}{\rho_f A_i} = \dfrac{\alpha_{ij}}{A_i}, \\ m_{ij-yx} = -\dfrac{F_{i-y}(a_j^x \equiv 1, a_j^y \equiv 0)}{\rho_f A_i} = \dfrac{\tau_{ij}}{A_i}, \\ m_{ij-xy} = -\dfrac{F_{i-x}(a_j^x \equiv 0, a_j^y \equiv 1)}{\rho_f A_i} = \dfrac{\sigma_{ij}}{A_i}, \\ m_{ij-yy} = -\dfrac{F_{i-y}(a_j^x \equiv 0, a_j^y \equiv 1)}{\rho_f A_i} = \dfrac{\beta_{ij}}{A_i}, \end{cases} \tag{2.5}$$

where A_i is the cross-area of the i-th section and can be calculated as

$$A_i = \iint\limits_{\mathcal{A}_i} dx \, dy.$$

These coefficients m_{ij-xx}, m_{ij-yx}, m_{ij-xy}, m_{ij-yy} are so-called mass coefficients, which implies that the motion of the j-th section can result in the added fluid inertia force not only on itself ($i = j$) but also on the other sections ($i \neq j$). The first and second variables to the right of the symbol '$-$' in the subscript represent the direction of the force and motion, respectively.

2.2. Application of source panel method

In the previous section we obtained the perturbation potential equation and its boundary conditions, and now we give the method for its numerical solution. The studied model and its discretization are shown in Fig. 1. The boundaries $\mathcal{B}_i$ ($i = 0, \ldots, N$) have been discretized into a set of panels. At the center of each panel, there is a control point. On the j-th panel, as shown in Fig. 2, we define a local coordinate at its middle point, namely (ξ, η). According to the panel method, a source distribution is considered along with this panel, and the source strength per length on this panel is assumed constant such that $\lambda_j(\xi) = \lambda_j =$ const. The induced velocities by the source distribution at the control points can be calculated by the integrations in terms of the source of intensity λ_j.

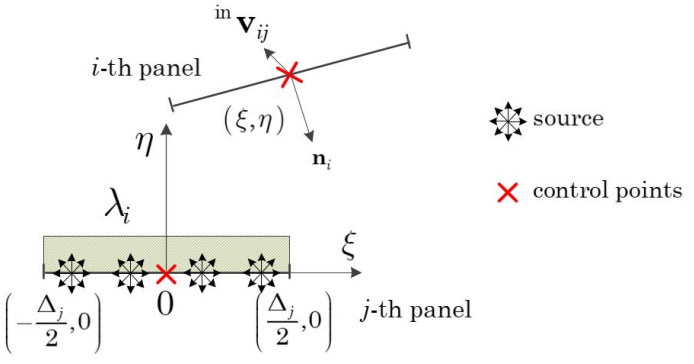

FIG. 2. Sketch of a panel model and its local coordinate system.

According to the superposition principle, the total flow induced-velocity at this control point by all panels is calculated as

$$ {}^{\text{in}}\mathbf{v}_i = \sum_{j=1}^{MN} {}^{\text{in}}\mathbf{v}_{ij} = \sum_{j=1}^{MN} {}^{\text{v}}\mathbf{C}_{ij}\lambda_j, \tag{2.6} $$

where $MN = \sum_{i=0}^{N} M_i$ is the total number of all panels, ${}^{\text{in}}\mathbf{v}_{ij}$ is the normal flow velocity at the control point of the i-th panel induced by the j-th panel, and ${}^{\text{v}}\mathbf{C}_{ij}$ is the influence coefficient of the normal fluid-induced velocity between panels i and j, and is defined as

$$
{}^{\mathrm{v}}\mathbf{C}_{ij} = \frac{\tilde{\mathbf{n}}_i}{2\pi} \cdot \begin{pmatrix} \int_{\frac{-\Delta_j}{2}}^{\frac{\Delta_j}{2}} \dfrac{\xi_i - \xi}{(\xi_i - \xi)^2 + \eta_i^2} d\xi \\ \int_{\frac{-\Delta_j}{2}}^{\frac{\Delta_j}{2}} \dfrac{\eta_i}{(\xi_i - \xi)^2 + \eta_i^2} d\xi \end{pmatrix}^T, \tag{2.7}
$$

where $\tilde{\mathbf{n}}_i$ is the unit normal vector of the i-th panel in the local coordinate system.

When the flow induced-velocities of all control points are obtained, the boundary condition of Eq. (2.2) can be specified at these points as

$$
({}^{\mathrm{in}}\mathbf{v})_{MN\times 1} = {}^{\mathrm{v}}\mathbf{C}_{MN\times MN} \times \Lambda_{MN\times 1} = (\mathbf{v}_B)_{MN\times 1}, \tag{2.8}
$$

where Λ is the vector of the strength of the source on all panels. The vector of the normal velocities $\mathbf{v}_B$ at all control points results by the motion of the j-th section, is defined as:

$$
\begin{aligned}
\mathbf{v}_B &= \begin{bmatrix} \mathbf{0}_{\left(\sum_{i=0}^{j-1} M_i\right)\times 1} \\ - - - - - - \\ \begin{bmatrix} \mathbf{v}_j \cdot \mathbf{n}_{j1} \\ \mathbf{v}_j \cdot \mathbf{n}_{j2} \\ \cdots \\ \mathbf{v}_j \cdot \mathbf{n}_{jM_j} \end{bmatrix} \\ - - - - - - \\ \mathbf{0}_{\left(\sum_{i=j+1}^{N} M_i\right)\times 1} \end{bmatrix} = \begin{bmatrix} \mathbf{0}_{\left(\sum_{i=0}^{j-1} M_i\right)\times 1} \\ - - - - - - \\ \begin{bmatrix} \mathbf{I}_x \cdot \mathbf{n}_{j1} \\ \mathbf{I}_x \cdot \mathbf{n}_{j2} \\ \cdots \\ \mathbf{I}_x \cdot \mathbf{n}_{jM_j} \end{bmatrix} \\ - - - - - - \\ \mathbf{0}_{\left(\sum_{i=j+1}^{N} M_i\right)\times 1} \end{bmatrix} \cdot v_j^x + \begin{bmatrix} \mathbf{0}_{\left(\sum_{i=0}^{j-1} M_i\right)\times 1} \\ - - - - - - \\ \begin{bmatrix} \mathbf{I}_y \cdot \mathbf{n}_{j1} \\ \mathbf{I}_y \cdot \mathbf{n}_{j2} \\ \cdots \\ \mathbf{I}_y \cdot \mathbf{n}_{jM_j} \end{bmatrix} \\ - - - - - - \\ \mathbf{0}_{\left(\sum_{i=j+1}^{N} M_i\right)\times 1} \end{bmatrix} \cdot v_j^y \\
&\triangleq \mathbf{B}_{j-x} \cdot v_j^x + \mathbf{B}_{j-y} \cdot v_j^y,
\end{aligned} \tag{2.9}
$$

where $\mathbf{n}_{jk} = (n_{jk}^x, n_{jk}^y)$ is the vector of the normal direction of the k-th panel on the boundary $\mathcal{B}_j$, and $\mathbf{I}_x = (1, 0)$, $\mathbf{I}_y = (0, 1)$.

From Eq. (2.8), the source strength vector of all panels is solved as

$$
\Lambda = {}^{\mathrm{v}}\mathbf{C}^{-1} \times \mathbf{v}_B, \tag{2.10}
$$

and then the fluid potential on boundary $\mathcal{B}_i$ is calculated as

$$
(\Phi_i)_{M_i\times 1} = {}^{\varphi}\mathbf{C}_{M_i\times MN} \times \Lambda_{MN\times 1} = {}^{\varphi}\mathbf{C} \times {}^{\mathrm{v}}\mathbf{C}^{-1} \times \mathbf{v}_B, \tag{2.11}
$$

where Φ_i is the potential vector of panels on $\mathcal{B}_i$, ${}^{\varphi}\mathbf{C}$ is the matrix of influence coefficients. ${}^{\varphi}\mathbf{C}_{ij}$ means the potential at i-th control point caused by the j-th panel and it is also evaluated in the local coordinate system of j-th panel as

$$ {}^{\varphi}\mathbf{C}_{ij} = \frac{1}{4\pi} \int_{-\Delta_j/2}^{\Delta_j/2} \ln[(\xi - \xi_i)^2 + \eta_i^2]\, d\xi. \tag{2.12} $$

Finally, the fluid pressure on the boundary $\mathcal{B}_i$ is solved as

$$ (\mathbf{p}_i)_{M_i \times 1} = -\rho_f \frac{\partial \Phi_i}{\partial t} = -\rho_f \cdot {}^{\varphi}\mathbf{C} \times {}^{\mathrm{v}}\mathbf{C}^{-1} \times \mathbf{a}_B \triangleq {}^{\mathrm{a}}\mathbf{C} \times \mathbf{a}_B, \tag{2.13} $$

where $\mathbf{p}_i$ is the vector of pressure at control points on the boundary $\mathcal{B}_i$, $\mathbf{a}_B$ is the vector of accelerations at all control points, which is defined as

$$ \mathbf{a}_B \triangleq \frac{d\mathbf{v}_B}{dt} = \mathbf{B}_{j-x} \cdot a_j^x + \mathbf{B}_{j-y} \cdot a_j^y. \tag{2.14} $$

Accordingly, the fluid force on the i-th section is then calculated from the following product, such that:

$$ \begin{cases} F_{i-x} = -\mathbf{s}_i^x \cdot \mathbf{p}_i = -\rho_f(\alpha_{ij} a_j^x + \tau_{ij} a_j^y), \\ F_{i-y} = -\mathbf{s}_i^y \cdot \mathbf{p}_i = -\rho_f(\sigma_{ij} a_j^x + \beta_{ij} a_j^y). \end{cases} \tag{2.15} $$

Then these four coefficients, $\alpha_{ij}, \sigma_{ij}, \tau_{ij}, \beta_{ij}$ given in Eq. (2.5) now can be rewritten as:

$$ \begin{cases} \alpha_{ij} = \mathbf{s}_i^x \cdot ({}^{\mathrm{a}}\mathbf{C} \times \mathbf{B}_{j-x}), \\ \sigma_{ij} = \mathbf{s}_i^y \cdot ({}^{\mathrm{a}}\mathbf{C} \times \mathbf{B}_{j-x}), \\ \tau_{ij} = \mathbf{s}_i^x \cdot ({}^{\mathrm{a}}\mathbf{C} \times \mathbf{B}_{j-y}), \\ \beta_{ij} = \mathbf{s}_i^y \cdot ({}^{\mathrm{a}}\mathbf{C} \times \mathbf{B}_{j-y}), \end{cases} \tag{2.16} $$

where the vectors $\mathbf{s}_i^x$ and $\mathbf{s}_i^y$ respectively stand for the projected length of the panels on the boundary $\mathcal{B}_i$ along the x and y directions, and are calculated as

$$ \begin{cases} \mathbf{s}_i^x = [n_{i1}^x \Delta l_{i1}, n_{i2}^x \Delta l_{i2}, \ldots, n_{iM_i}^x \Delta l_{iM_i}]^T, \\ \mathbf{s}_i^y = [n_{i1}^y \Delta l_{i1}, n_{i2}^y \Delta l_{i2}, \ldots, n_{iM_i}^y \Delta l_{iM_i}]^T, \end{cases} \tag{2.17} $$

where Δl_{ik} is the length of the k-th panel on the boundary $\mathcal{B}_i$.

Finally, by substituting the results of Eq. (2.16) into Eq. (2.5), the four added mass coefficients are completely determined. It should be pointed out that, like in the literature such as [3, 18, 19], to simplify the analysis, only one direction of acceleration is considered. Hence in the following discussion, we only take into account the mass coefficients about the acceleration in the x-direction. Consider the first two lines of Eq. (2.16) and define the following simple formulation with neglecting the left superscript; thus, we obtain

$$ \begin{cases} m_{ij-xx} = \dfrac{\mathbf{s}_i^x \cdot ({}^{\mathrm{a}}\mathbf{C} \times \mathbf{B}_{j-x})}{A_i}, \\ m_{ij-yx} = \dfrac{\mathbf{s}_i^y \cdot ({}^{\mathrm{a}}\mathbf{C} \times \mathbf{B}_{j-x})}{A_i}. \end{cases} \tag{2.18} $$

When $i = j$, these above coefficients stand for the added fluid force on the i-th section caused by its own motion and are called the added mass conferences; and the coefficients for $i \neq j$ refer to the added fluid force caused by the motions of other sections and are called the coupling mass coefficients.

3. Verification and discussion

3.1. Comparison with other theories

To verify the accuracy and discuss the applicability of the present numerical method, we apply it for some typical problems and also compare with other theories and software. With no loss of generality, firstly we consider the following three simple and typical cases in Fig. 3, whose added mass coefficients have been calculated or approximated by theoretical methods.

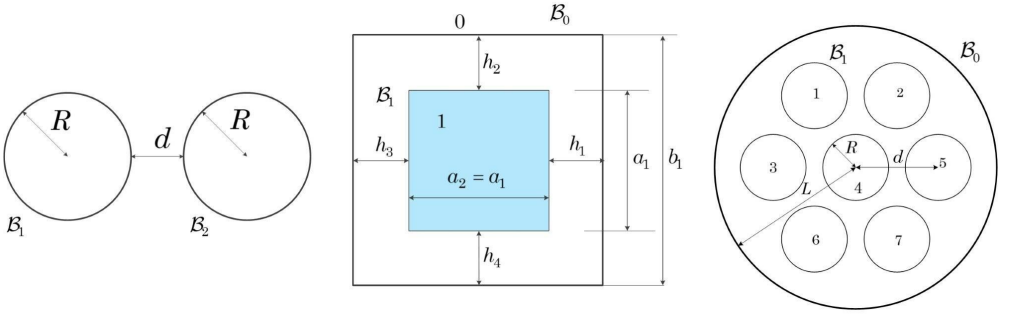

(a) (b) (c)

FIG. 3. Examples for verification. (a) Two circular sections in an infinite fluid. (b) Two coaxial squares. (c) A group of circular sections in a cylindrical container. These three examples are the case that the section has a single boundary.

As shown in Fig. 3(a), in the first example, there are two circular sections in an open fluid [20]. These two circular cylinders have the same radius R, and the distance between them is d. The boundaries of this model are $\mathcal{C}^1$ continuity and the outer container is absent, i.e., it is the case of an open flow. As for this classic problem, [20] presented a theoretical analysis, and the coefficients m_{11-xx} is calculated as

$$m_{11-xx} = 1 + 4\sinh^2\alpha \sum_{n=1}^{\infty} \frac{n e^{-n(2\alpha+\beta)}}{\sinh(n\beta)}, \tag{3.1}$$

where

$$\alpha = \ln\left(\frac{P}{2R} + \sqrt{\left(\frac{P}{2R}\right)^2 - 1}\right), \qquad \beta = \ln\left(\frac{P^2 - 2R^2}{2R^2} + \sqrt{\left(\frac{P^2 - 2R^2}{2R^2}\right)^2 - 1}\right),$$

and $P = d + 2R$ is the distance between the centers of two circular cylinders.

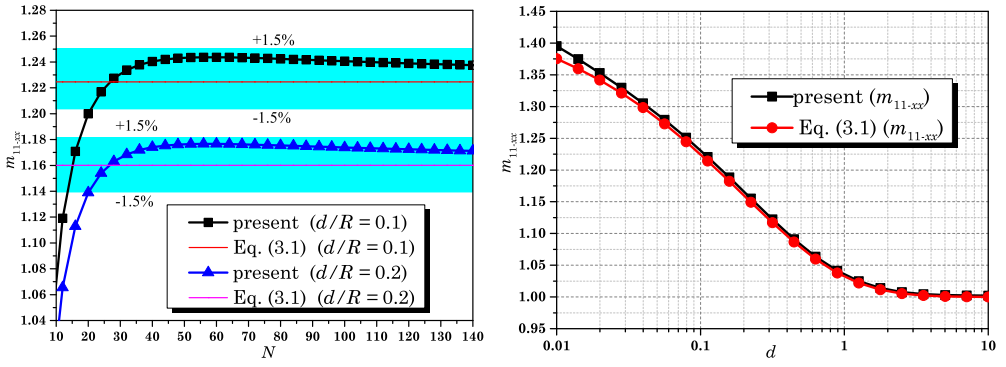

(a) (b)

FIG. 4. Examination on the convergence of the present method. (a) Results of mass coefficient in terms of panel number. (b) Comparison of the present method and Eq. (3.1).

In the present numerical calculation, the circumference is divided into N parts evenly. The convergence of the present method is evaluated in Fig. 4(a), where m_{11-xx} is plotted in terms of N for various ratios of d/R, $(R = 1)$. From Fig. 4(b), it is seen that for the different ratios of d/R, m_{11-xx} firstly increases sharply with increasing N. The growth rate decreases gradually, then slowly decays with increasing N and converges to the analytical solution calculated by Eq. (3.1a). Though the convergence rate is slow when $N > 24$, all relative errors between the present method and the analytical solution are less than 1.5%, showing the accuracy of the present method. (In the following numerical examples, we have all performed such a convergence analysis, and the further discussion is carried out after the convergence guaranteed). The comparison of the present method and Eq. (3.1) for various d is shown in Fig. 4(b). From this comparison, it is seen that the present results are in good agreement with the theoretical ones. The accuracy of the present method for calculating the added mass coefficient of a cylindrical section in an infinite fluid is verified. In addition, Fig. 4(b) shows that as d increases, m_{11-xx} decreases, because the other cylinder will stagnate the flow line, resulting in an increase of fluid pressure, which becomes more pronounced as d decreases.

Next, we discuss the added mass coefficient of structure in confined fluid. As shown in Fig. 3(b), we consider a square section in an outer square container. This interesting model is used to model spent fuel storage racks submerged in the water contained in a pool and studied in [21]. Note that these boundaries of sections are only $\mathcal{C}^0$ continuity, leading difficulties in the mathematical analysis so that the traditional series solution [5] is no longer applicable. In [21], the added mass coefficient on the inner square can be approximated evaluated as

$$m_{11-xx} = \left(\frac{a_1}{12h_1} + \frac{a_1}{12h_3} + \frac{a_2}{4h_2} + \frac{a_2}{4h_4} \right). \tag{3.2}$$

To facilitate this discussion, we assume that the four gaps have the same values ($h_1 = h_2 = h_3 = h_4 = h_0$), and Fig. 5 shows the dependence of m_{11-xx} on h_0. It is seen that when $h_0 < 0.1$, the present numerical results are in good agreement with Eq. (3.2); however, as h_0 further increases, the difference between them is continually growing. When h_0 is relatively large, say, $h_0 \gg 1$, the present numerical result is approaching the theoretical value $m_{11-xx} = 1.186$, and this is consistent with the conclusion in [6]. But the result of Eq. (3.2) is $m_{11-xx} = 0$ and this is clearly incorrect because this means that the structure is not influenced by the fluid. In fact, as [21] emphasized, Eq. (3.2) is only applicable when h is small. Those results mean that this method is also accurate for the calculation of the added mass coefficient of the section in the boundary fluid and is more applicable than Eq. (3.2).

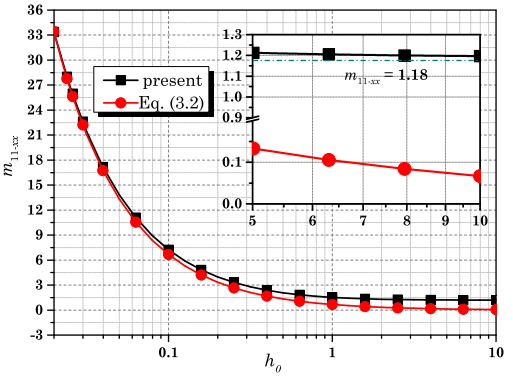

FIG. 5. Results of mass coefficients in terms of h_0 and the comparison with Eq. (3.2).

In the previous two examples we discussed single and two sections, to further discuss the applicability of this method we consider the case of multiple sections. As shown in Fig. 3(c), there is a group of circular sections in a cylindrical container, this model can be found in the steam generator [1]. Each circular section refers to a separated pipe, implying that all sections can undergo independent motions. The boundaries of a steam generator are $\mathcal{C}^1$ continuity, and a series solutions for the added coefficients was firstly proposed by CHEN [5]. We also applied the present numerical method for such a classical problem, and following [22] the parameters are specified as $R = 3.3\,\text{mm}$, $d = 8.28\,\text{mm}$, and $L = 14.1566\,\text{mm}$. Due to this model's symmetry, only the added mass coefficients in Sections 1, 3, and 4 are discussed here. Figure 6 shows that the present numerical results are in good agreement with the theoretical solutions. One section's motion often causes mass coefficients in both the x- and y-directions. Interestingly, the sum of mass coefficients in the x- and y-directions for these three sections are evaluated in Table 1 and compared with the results calculated by the method in [5] and

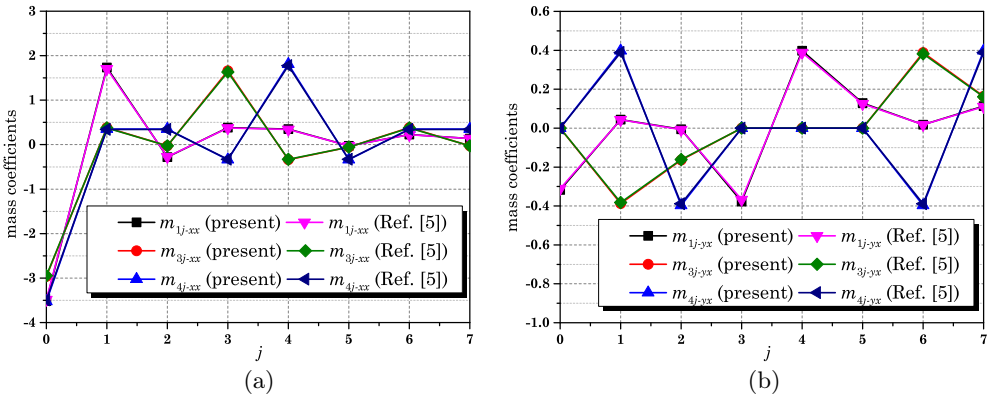

FIG. 6. Results of mass coefficients and the comparison with [5].

TABLE 1. The sums of mass coefficients and the comparison with [5].

Cases	$\sum_{j=0}^{7} m_{ij-xx}$			$\sum_{j=0}^{7} m_{ij-yx}$		
i	1	3	7	1	3	7
Present	−0.9912	−0.9925	−0.9912	−0.0008	0	0
CHUNG [5]	−0.9998	−0.9997	−0.9997	−0.0001	0	0

good agreement between them can be observed. These results are also consistent with the conclusion in [23] that the sum of the added mass coefficients of other sections along the motion direction caused by a section's motion is equal to the constant value −1, and the sum of the coefficients perpendicular to the motion is the constant value 0. It is worth noting that the continuity characters of boundaries of those sections in Figs. 3(b) and 3(c) are different; however, the present method shows good applicability; that is one of its most important advantages.

3.2. Comparison with software

In Fig. 3, these sections generally have only a single section, and this is a simple case that can be analyzed by a theoretical method. In order to further discuss the applicability of the present method, next, we consider the case of a group of motion-dependent sections in a confined fluid. As shown in Fig. 7(a), now we perform a numerical computation to the single fuel assembly in the pressurized water reactor (PWR). This model can be simplified as a group of sections in a fluid confined by four core baffles. The PWR fuel assembly consists of a 17×17 array of 264 fuel rods, 24 control rod guide tubes, and one instrumentation tube; due to an actual model's complexity, a 6×6 fuel rods array mock-ups are taken to simulate the fuel assembly in [24]. Unlike the motion-independent sections in Fig. 3(c), these sections are all connected to a rigid grid (the dashed rect-

angular) and will undergo the same motion. In this situation, the inner section boundary is not a single boundary as the above two cases, it should be a group of circle boundaries. The model is complex, and it is not easy to solve the added mass coefficients by a theoretical method. We solve these mass coefficients using the commercial software ANSYS and FLUENT. A comparison of results applies to validate the accuracy of the present method.

The details of the simplified model of a fuel assembly is shown in Fig. 7(a). In the area with dashed lines, there is a fuel assembly containing 36 fuel rods of a circular cross-section. The fuel rod diameters and the distance between the centers of rod are $R = 4.75\,\text{mm}$ and $d = 12.6\,\text{mm}$, respectively. We calculate this model by both present method and software for a comparison. The finite element model in ANSYS is shown in Fig. 7(b), in which the assembly is discretized by the PLANE42 element and the fluid is discretized by the FLUID29 element. All the degrees of freedom of the nodes on assembly are coupled into one degree of freedom. The assembly is connected to a fixed point by a linear spring (COMBIN14 element) and its density is set as ρ_a.

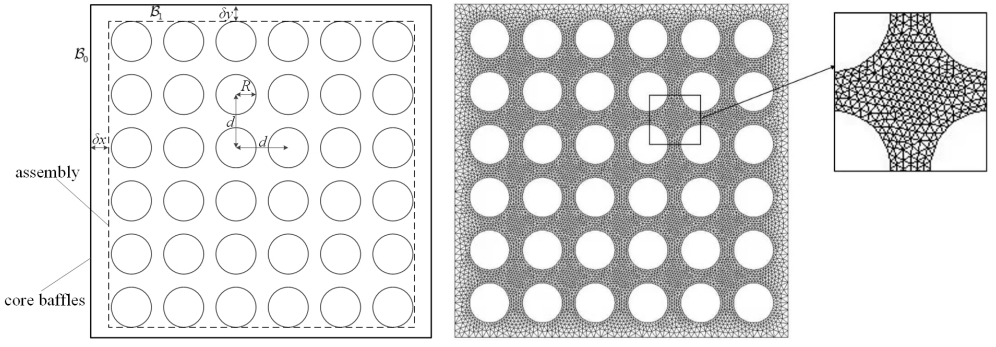

(a) (b)

FIG. 7. The verification example of a PWR fuel assembly. (a) The simplified mechanical model. (b) The computational model in ANSYS. In this case the section boundary is a group of circle boundaries.

The following is a brief description of the scheme, we calculated the mass coefficients from this software. Firstly, we set the fluid density to 0 (i.e., there is no fluid) and denote the calculated frequency as f_a. And then, we set the fluid as ρ_w and denote the calculated frequency as f_w. Then according to vibration mechanics, the added mass coefficient can be expressed as

$$m_{11-xx} = \frac{\rho_a}{\rho_w}\left(\frac{f_a^2}{f_w^2} - 1\right). \tag{3.3}$$

In ANSYS, we set $\rho_a = \rho_w$ to simplify the calculation.

The results of the added mass coefficient of the assembly with different gaps are compared in Fig. 8(a). For the different gaps between the fuel assembly and four core baffles, the relative error between the results calculated by the two methods is less than 2%, implying that this method is effective. The results calculated by present and ANSYS show a conclusion that may be counterintuitive for many people: the gap perpendicular to the direction of motion has a more significant effect on the added mass coefficient of the fuel assembly. In fact, we can also draw the same conclusion from the added mass coefficients of a spent fuel rack given in Eq. (3.2). Equation (3.2) shows that the gap perpendicular to the motion direction (h_2 and h_4) has a greater influence than others (h_1 and h_3). To qualitatively explain this phenomenon, we discuss a simple mode in Fig. 8(b). A cylinder section is located in the fluid enclosed by four baffles, and the cylinder radius is 1 m while the gap between the cylinder and baffle in the direction of the cylinder motion is 0.1 m. The length and width of the rectangular fluid field are 10 m and 2.2 m, respectively. We set the cylinder boundary with a given velocity $V = 0.001\,\mathrm{m/s}$, and the flow field and pressure distribution for such a given velocity boundary are then calculated by using FLUENT.

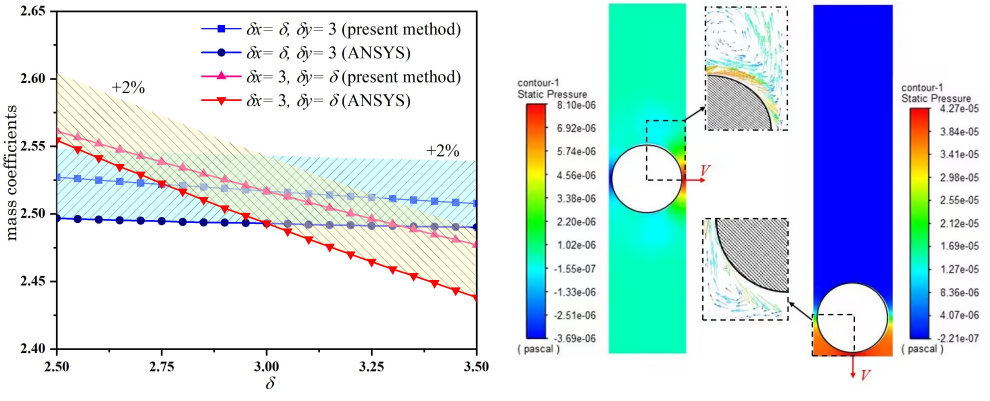

(a) (b)

FIG. 8. (a) Mass coefficients in terms of gaps and the comparison with ANSYS. (b) Velocity vectors and pressure comparison for a simplified model.

The velocity vectors of the flow are shown in Fig. 8(b). It is seen that when the gap perpendicular to the direction of motion is large (the left one), the fluid can outflow from the gap, so the pressure is relatively small. However, when the gap is small (the right one), it is not easy for the fluid to outflow, leading to a larger pressure. It is worth noting that the computational complexity of the present method is much smaller than that of ANSYS. For the fuel assembly model in Fig. 7, when $\delta x = \delta y = 3\,\mathrm{mm}$, 101800 elements are needed for ANSYS modeling while in the present discrete models, only 1156 panels are used, and

it means the present numerical method is more efficient. In this model, the boundaries of fuel assembly are $\mathcal{C}^1$ while those of core baffles are $\mathcal{C}^0$, and this indicates the good applicability of the present method to complex boundaries.

The last problem we examined is shown in Fig. 9(a), and its discrete model calculated by FLUENT is shown in Fig. 9(b). This model extends the case of Fig. 7(a) from one to three assemblies. There is a 1×3 array of 108 fuel rods of circular sections, which is also a classical model in the nuclear engineering design. Following the practical engineering problem, the fuel assemblies are assumed to be placed parallel to each other in a closed liquid. Each fuel assembly (the gray square in Fig. 9(a)) consists of an array of 36 rods, as shown in the circle sections in the square with dash lines in Fig. 7(a). The distance between two fuel assemblies is $\delta = 3.94\,\text{mm}$, and the gaps between fuel assembly and core baffles are $\delta x = \delta y = 2.67\,\text{mm}$). Different from the model in Fig. 7, each assembly or baffles, moving independently, will lead to fluid forces not only on itself but also on other assemblies. We also calculated this problem by both the present method and FLUENT. The fluid is set as unsteady and inviscid in FLUENT, and the dynamic mesh technology is used. Specify the motion of the assembly or baffles with a constant acceleration in the horizontal direction and extract the total forces acting on the assemblies. Use these forces to divide the constant acceleration and the weight of the assembly discharging fluid, and then the mass coefficients can be obtained.

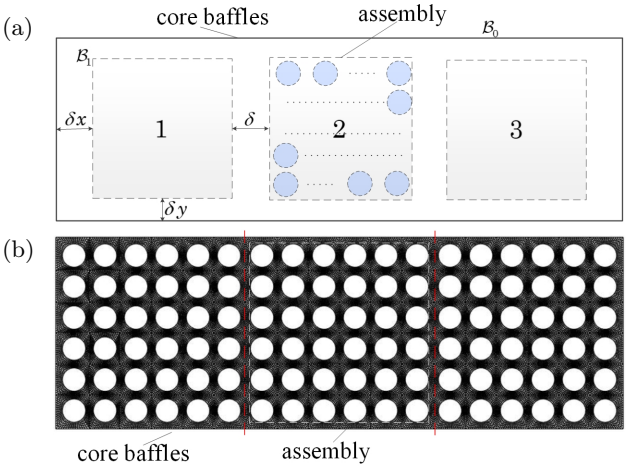

FIG. 9. The verification example of 1×3 PWR fuel assemblies. (a) The simplified mechanical model. (b) The computational model in FLUENT.

The results of mass coefficients calculated by the present method and FLUENT are compared and shown in Table 2, where the subscript "0" stands for the core baffles. The present method and software results well agree, and the

maximum relative error is less than 3%. The error of the model in Fig. 7 is more significant than that of the model in Fig. 6; this may be because the transient calculation in FLUENT is not as accurate as the modal calculation in ANSYS. The same model as the single fuel assembly model in Fig. 7 also contains both the $\mathcal{C}^1$ and $\mathcal{C}^0$ boundaries. These examples examined in this section show that the present panel method is accurate and effective for the calculations of mass coefficients. The present numerical method can provide some references for mass coefficient calculations of other engineering structures.

Table 2. Results of the present method and a comparison with FLUENT.

Added mass coefficients	m_{10-xx}	m_{11-xx}	m_{20-xx}	m_{22-xx}	m_{30-xx}	m_{33-xx}
Present	−3.561	2.508	−3.612	2.642	−3.561	2.508
FLUENT	−3.479	2.541	−3.644	2.629	−3.479	2.541
error (%)	−2.357	−1.298	0.878	0.494	−2.357	−1.298

4. Summary

For the long columnar structures commonly found in engineering, this paper reports a numerical study on the added mass of structures with complex sections in the fluid. The boundaries of structures are firstly discretized into several panels, and constant sources are set on each panel to satisfy the boundary conditions. Then the influence matrix is obtained by the singular integral. The fluid pressure on these panels is calculated using the influence matrices and the motions of a specified boundary. Finally, the mass coefficients are calculated as the quotient of fluid forces acting on sections and the mass of fluid displaced by these sections.

This paper developed an efficient and accurate numerical solution based on the two-dimensional source panel method. We use the present method to calculate the added masses of five typical structures and compare with other methods. The results show the accuracy and efficiency of the method. This method has the wide applicability, whether the fluid is bounded or not, the boundaries are $\mathcal{C}^0$ or $\mathcal{C}^1$ continuity, and the section with a single boundary or a group of boundaries. Its applicability and simplicity make it an effective tool for other related engineering problems.

Acknowledgements

This work is supported by the National Natural Science Foundation of China (Grant Nos: 12072298; 12172311).

Conflict of interest

The authors declare that they have no conflict of interest.

References

1. M.P. Paidoussis, S. Suss, M. Pustejovsky, *Free vibration of clusters of cylinders in liquid-filled channels*, Journal of Sound and Vibration, **55**, 3, 443–459, 1977, doi: 10.1016/S0022-460X(77)80025-4.
2. S. Yoshimura, K. Kobayashi, H. Akiba, *Seismic response analysis of full-scale boiling water reactor using three-dimensional finite element method*, Journal of Nuclear Science and Technology, **52**, 4, 546–567, 2015, doi: 10.1080/00223131.2014.963000.
3. A. Wanninger, M. Seidl, R. Macian-Juan, *Mechanical analysis of the bow deformation of a row of fuel assemblies in a PWR core*, Nuclear Engineering and Technology, **50**, 2, 297–305, 2018, doi: 10.1016/j.net.2017.12.009.
4. R.J. Fritz, *The effect of liquids on the dynamic motions of immersed solids*, Journal of Engineering for Industry, **94**, 1, 167, 1972, doi: 10.1115/1.3428107.
5. H. Chung, S.S. Chan, *Vibration of a group of circular cylinders in a confined fluid*, Journal of Applied Mechanics, **99**, 2, 455–455, 1977, doi: 10.1115/1.3424026.
6. R.G. Dong, *Effective Mass and Damping of Submerged Structures*, (No. UCRL-52342) California University, Livermore, USA, Lawrence Livermore Laboratory, 1978, doi: 10.2172/7038325.
7. K.H. Jeong, M.J. Jhung, *Added mass estimation of square sections coupled with a liquid using finite element method*, Nuclear Engineering and Technology, **49**, 1, 234–244, 2017, doi: 10.1016/j.net.2016.07.010.
8. W. Li, D. Lu, Y. Liu, *Numerical investigation on the fluid added mass of spent fuel storage rack*, Nuclear Engineering and Design, **339**, 83–91, 2018, doi: 10.1016/j.nucengdes.2018.08.025.
9. Jr. J.D. Anderson, *Fundamentals of Aerodynamics*, McGraw-Hill Education, New York, 2010.
10. H.N.V. Dutt, S.R. Rajeswari, *Wing-body interference using a hybrid panel method*, Acta Mechanica, **106**, 3-4, 111–126, 1994, doi: 10.1007/BF01213557.
11. M.S. Tarafder, K. Suzuki, *Numerical calculation of free-surface potential flow around a ship using the modified Rankine source panel method*, Ocean Engineering, **35**, 5-6, 536–544, 2008, doi: 10.1016/j.oceaneng.2007.11.004.
12. E. Yari, H. Ghassemi, *Boundary element method applied to added mass coefficient calculation of the skewed marine propellers*, Polish Maritime Research, **2**, 90, 25–31, 2016, doi: 10.1515/pomr-2016-0017.
13. J. Katz, *Aerodynamics of race cars*, Annual Review of Fluid Mechanics, **38**, 27–63, 2006, doi: 10.1146/annurev.fluid.38.050304.092016.
14. A.D. Lucey, P.W. Carpenter, *A numerical simulation of the interaction of a compliant wall and inviscid flow*, Journal of Fluid Mechanics, **234**, 121–146, 1992, doi: 10.1017/S0022112092000727.

15. D.L. ASHBY, *Development and validation of an advanced low-order panel method*, NASA TM-101024, 1988.

16. I.S. SAHIN, J.A. CRANE, K.E. WATSON, *Added mass coefficients for submerged bodies by a low-order panel method*, Transaction of the ASME, **115**, 234, 452–456, 1993, doi: 10.1115/1.2910159.

17. J. KATZ, A. PLOTKIN, *Low-speed Aerodynamics*, Cambridge University Press, Cambridge, 2001.

18. K.H. JEONG, M.J. JHUNG, *Added mass estimation of square sections coupled with a liquid using finite element method*, Nuclear Engineering and Technology, **49**, 1, 234–244, 2017, doi: 10.1016/j.net.2016.07.010.

19. J. STABEL, M. REN, *Fluid-structure-interaction for the analysis of the dynamics of fuel storage racks in the case of seismic loads*, Nuclear Engineering and Design, **206**, 2-3, 167–176, 2001, doi: 10.1016/S0029-5493(00)00431-3.

20. V.Y. MAZUR, *Motion of two circular cylinders in an ideal fluid*, Fluid Dynamics, **5**, 6, 969–972, 1970, doi: 10.1007/BF01015098.

21. Y. LIU, D. LU, Y. WANG, H. LIU, *The sliding and overturning analysis of spent fuel storage rack based on dynamic analysis model*, Science and Technology of Nuclear Installations, 2016, doi: 10.1155/2016/8368504.

22. R. GAJAPATHY, K. VELUSAMY, P. SELVARAJ, P. CHELLAPANDIS, *CFD investigation of helical wire-wrapped 7-pin fuel bundle and the challenges in modeling full scale 217 pin bundle*, Nuclear Engineering and Design, **237**, 24, 2332–2342, 2007, doi: 10.1016/j.nucengdes.2007.05.003.

23. D. ZHANG, P. LI, Q. WANG, Y. YANG, *A note on added mass of a group of sections in confined fluid: a general conclusion*, Archive of Applied Mechanics, **91**, 11, 4433–4439, 2021, doi: 10.1007/s00419-021-02050-9.

24. J. RIGAUDEAU, D. BROCHARD, A. BENJEDIDIA, *Fluid structure interaction in the response of PWR fuel assemblies to horizontal seismic loads*, Structural Mechanics in Reactor Technology, **12**, 121–126, 1993.

Received May 21, 2022; revised version December 28, 2022.
Published online February 24, 2023.